

Alternate-day fat diet and exenatide modulate the brain leptin JAK2/STAT3/SOCS3 pathway in a fat diet-induced obesity and insulin resistance mouse model

Mona K. Tawfik¹, Dahlia I. Badran^{2,3}, Mohammed M. Keshawy⁴, Samy Makary⁵, Mohamed Abdo⁵

¹Department of Pharmacology, Faculty of Medicine, Suez Canal University, Ismailia, Egypt

²Department of Biochemistry, Faculty of Medicine, Suez Canal University, Ismailia, Egypt

³Department of Biochemistry, Faculty of Medicine, Badr University, Cairo, Egypt

⁴Department of Internal Medicine, Nephrology Division, Faculty of Medicine, Suez Canal University, Ismailia, Egypt

⁵Department of Physiology, Faculty of Medicine, Suez Canal University, Ismailia, Egypt

Submitted: 3 December 2022; **Accepted:** 24 December 2022

Online publication: 1 February 2023

Arch Med Sci 2023; 19 (5): 1508–1519

DOI: <https://doi.org/10.5114/aoms/158534>

Copyright © 2023 Termedia & Banach

Corresponding author:

Dahlia I. Badran
Department of Biochemistry
Faculty of Medicine
Suez Canal University
Ismailia 41522, Egypt
Department of Biochemistry
Faculty of Medicine
Badr University
Cairo, Egypt
Phone: 002-01222424174
E-mail: dalia_badran@med.suez.edu.eg

Abstract

Introduction: Obesity is one of the most burdensome health problems and is closely linked to leptin resistance. The study examined whether an alternate-day high-fat diet (ADF) and/or GLP-1 agonist (exenatide) modulate brain leptin resistance caused by a high-fat diet (HFD).

Material and methods: Sixty adult male mice were divided into 6 groups: (i) normal palatable diet (NPD), (ii) exenatide control (NPD received exenatide) (iii) HFD, (iv) ADF treated, (v) exenatide treated, (vi) ADF and exenatide treated. All animal groups were fed a HFD for 8 weeks, before they received treatment (ADF and/or exenatide) for 8 additional weeks. Body weight was assessed at the start and at the end of the experiment. Lipid profile, brain leptin and its receptor expression with the leptin-sensitive pathway, JAK2/STAT3/SOCS3/PTP1B, fasting blood glucose (FBG), serum insulin, liver metabolic handling via its regulators IRS1/PI3K/GLUT4 for hyperinsulinemia/obesity-induced *PDK3/NAFLD2* modification, and liver enzymes were determined at the end of the experiment.

Results: ADF and exenatide reduced body weight and FBG in HFD-obese mice ($p < 0.05$). The combined ADF and exenatide regimen enhanced the brain anorexic leptin/JAK2/STAT3 and attenuated the SOCS3/PTP1B pathway ($p < 0.05$). The ADF/exenatide anorexigenic brain effect also modulated liver glucose via IRS1/PI3K/GLUT4 expression ($p < 0.05$), attenuating *NAFLD2* and *PDK3* expression ($p < 0.05$). Liver enzymes and the histopathological profile confirmed the improvement.

Conclusions: In HFD caloric consumption, a combination of ADF and GLP-1 agonist enhances the brain leptin anorexigenic effect with the improvement of the metabolic sequelae of hyperinsulinemia, hyperlipidemia and liver steatosis.

Key words: leptin, hyperinsulinemia, alternate-day high-fat diet, high-fat diet, exenatide.

Introduction

Obesity is a leading health problem worldwide, which is associated with leptin resistance, insulin resistance, and hyperlipidemia [1].

It has been reported that the HFD is associated with metabolic disorders (weight gain, insulin and leptin resistance), disturbed serum profiles (hyperglycemia, hyperinsulinemia, hypercholesterolemia, hypertriglyceridemia) and abnormal liver aminotransferase activity as well as histopathological changes (hepatic steatosis and pericentral fibrosis) similar to humans with the non-alcoholic susceptibility gene NAFLD phenotype [2, 3].

The administration of a high-fat diet for 24 h could result in a change in glucose metabolism, triggering a reduced level of circulating leptin and thus contribute to a high-fat diet in promoting weight gain [4].

Leptin resistance is defined as decreased leptin receptor sensitivity with a consequent reduction in leptin appetite suppression and subsequent obesity [1].

The binding of leptin to its receptor in the hypothalamus enhances the Janus kinase JAK2/signal transducer and activator of the transcription (JAK2/STAT3, anorectic signal) signaling pathway inducing a satiety state, through activating cytokine signaling 3 suppression (SOCS3) that ends the leptin signaling effect on JAK2/STAT3 by terminating the JAK2 activity through ubiquitination [5]. Therefore, abnormal food intake is a state of disturbance of the suppressor SOCS3 effect on leptin-JAK2/STAT3 signaling [6, 7].

Protein tyrosine phosphatase 1B (PTP1B) is another negative regulator of leptin via dephosphorylation of the upstream activator molecules JAK2 and STAT3, representing the direct substrate of PTP1B [8].

Obesity and insulin resistance are targeted by glucagon-like peptide-1 (GLP-1) receptor agonists (exenatide; exendin-4) the common standard therapy used for hyperglycemia [9]. The liver is one of the primary target organs for GLP-1 agonists to exert their plasma-lowering effect in hyperglycemia via the insulin-regulated glucose transporter GLUT4 [10]. GLUT4 regulates body adiposity through crosstalk genes between leptin and insulin signaling promoting GLUT4 translocation and glucose transport in an insulin receptor substrate-1 (IRS-1)/phosphatidylinositol 3-kinase (PI3K) dependent manner [11].

According to our knowledge, no previous studies have investigated the effect of ADF and/or exenatide on the brain leptin signaling pathway and leptin resistance.

Pyruvate dehydrogenase kinase isoenzyme 3 (PDK3), which is a part of the pyruvate dehydrogenase complex (PDC), and the non-alcoholic susceptibility 2 gene (*NAFLD2*) are two novel adipogenesis regulators that have an apparent role in the pathogenesis of obesity and could contribute to liver steatosis [12, 13]. However, no study has

reported the effect of ADF and/or exenatide on their expression in HFD-induced liver steatosis.

The objective of the present study is to investigate the effects of ADF and/or exenatide, administered once daily for 8 weeks to mice with HFD-induced obesity and insulin resistance, on brain leptin resistance, insulin sensitivity and hepatic steatosis.

Material and methods

Experimental animals

Sixty male Swiss mice (22 ± 4 g) were purchased from Vacsera (Egypt). The Research Ethics Committee approved the protocol of the present study at the Faculty of Medicine, Suez Canal University with approval number 4264 according to the National Institute of Health Guide (National Institute of Health Publications No. 80-23, Revised 1978) for the care and use of laboratory animals for the experimental procedure.

Drugs and chemicals

Exenatide injection (BYDUREON vials (2 mg/2 ml solution), AstraZeneca Pharmaceuticals, Wilmington, DE, USA) was diluted with sterile saline [14].

Dietary protocols

HFD was used to induce obesity and insulin resistance [2]. Animals were fed the HFD for 8 weeks (Supplementary Figure S1 B). The HFD composition was as follows (g/kg): powdered NPD 365, lard 310, casein 250, cholesterol 10, vitamin and mineral mix 60, as described previously [15–17]. Mice subjected to ADF received NPD alternating with HFD, every other day, modified from Smith *et al.* [18].

Experimental design

The mice ($n = 60$) were randomly divided into 6 groups ($n: 10/\text{group}$) and assigned to groups as follows: Group (i): mice fed with NPD. Group (ii) exenatide control (NPD mice received exenatide, 10 µg/kg, s.c.) [14]. Group (iii) HFD control, mice fed HFD [18]. Group (iv) ADF treated mice fed ADF regime: (NPD/ADF) every other day. On day 1 they received as much HFD food as desired during the entire 24-h period. On day 2 they received NPD food and so on [18]. Group (v) exenatide treated, HFD mice received exenatide (HFD + exenatide, 10 µg/kg, s.c.) [14]. Group (vi) ADF and exenatide treated, HFD mice fed on ADF regimen and received exenatide (ADF + exenatide, 10 µg/kg, s.c.). All animal groups were fed the HFD for 8 weeks before they received the corresponding treatment (ADF and/or exenatide) for 8 additional weeks (Figure 1 A).

For exenatide groups, drug administration was every 24 h. Body weight was measured at the start and at the end of the study.

Serum levels of sugar and insulin resistance

FBG was tested using (Bio diagnostics, Cairo, Egypt) with an automated analyzer (Cobas 6000, Cobas c501, Roche).

Serum fasting insulin level was determined by an ELISA mouse kit (catalog #90080; Crystal Chem, Downers Grove, IL). Insulin resistance was determined using the Homeostatic Model Assessment of Insulin Resistance (HOMA-IR) index, which was calculated according to the formula: fasting insulin ($\mu\text{U/l}$) \times fasting glucose (nmol/l)/22.5 [19].

Blood and tissue sample collection

At the end of the study, sera were collected from anesthetized mice (80 mg/kg ketamine HCL, i.p.) and stored at -80°C until further assayed. Serum samples were tested for activities of the liver enzymes alanine aminotransferase (ALT) and aspartate aminotransferase (AST) and lipid profile was measured with a spectrophotometer. Then, brain and liver biopsies were taken, one part from which was fixed in neutral formalin 10% (v/v) and then paraffin-embedded for further histopathology and immunohistochemistry. Other parts of the brain and liver biopsies were processed for real-time polymerase chain reaction (qRT-PCR), western blotting, and ELISA assays [20].

Assessment of brain leptin level

Brain tissue was homogenized and centrifuged using the supernatant to assess leptin content by ELISA kit (Elabscience Biotechnology, USA, Catalog #: MBS012834).

Estimation of brain leptin receptor and liver *PDK3*, *GLUT4* and *NAFLD2* genes' expression by qRT-PCR

Expression profiling of brain leptin receptor (F: 5'-AGA ATT GTT CCT GGG CAC AAG -3'; R: 5'-ACACTCATCCTCACAGGTCC-3'), and liver *PDK3* (F: 5'-TGGAGATGGTGCCGCTAATG-3'; R: 5'-TGTGGTGTGATTGAGCAAC-3'), *GLUT4* (F: 5'-GAGCC-TGAATGCTAATGGAG-3'; R: 5'-GAGAGAGAGCGTCC-AATGTC-3'), and *NAFLD2* (F: 5'-GCCAGTACTGTC-CTCTCTTG-3'; R: 5'-CCCTGGGCAGCTATGTTTAT-3') genes was carried out using qRT-PCR following the guidelines of the Minimum Information for Publication of Quantitative Real-Time PCR Experiments (MIQE). All reactions were run using SYBR Green Master Mix (Applied Biosystems) under the following thermal cycling parameters: 95°C for

10 min (1 cycle), 95°C for 15 s, and 60°C for 1 min (40 cycles). Gene-specific primer pairs were designed with Gene Runner Software (Hasting Software, Inc., Hasting, NY) from RNA sequences from the gene bank as described previously [16].

Relative expression of studied gene mRNA was calculated using the comparative $2^{-\Delta\Delta\text{Ct}}$ method of analysis as described by Livak and Schmittgen [21]. All values were normalized to β -actin, which was used as the control housekeeping gene, and reported as fold change over background levels detected in the diseased groups. [16].

Estimation of brain JAK2, STAT3, SOCS3, PTP1 and liver IRS-1 and PI3K protein expression by Western blot technique

The brain JAK2, STAT3, SOCS, PTP1B proteins, and the liver IRS-1 and PI3K proteins were assessed by Western blot technique achieved by extraction from tissue homogenates using ice-cold radioimmunoprecipitation assay (RIPA), using the V3 Western Workflow Complete System, Bio-Rad Hercules, (CA, USA) as described previously [22]. Protein bands were visualized using enhanced chemiluminescence (Pierce ECL Western blotting substrate) and Alliance gel doc (Alliance 4.7 Gel doc, UK). UV Tec software (UK) was used to semi-quantify protein bands. All protein bands were normalized against β -actin protein. Band intensity was analyzed by the ChemiDoc imaging system with Image Lab TM software version 5.1 (Bio-Rad Laboratories Inc., Hercules, CA, USA).

Lipid profile and liver enzymes

The serum total cholesterol (TC), triglycerides (TG), low-density lipoprotein cholesterol (LDL), and high-density lipoprotein cholesterol (HDL) were measured by the enzymatic colorimetric method [23, 24], and the liver enzymes alanine aminotransferase (ALT) and aspartate aminotransferase (AST) were measured by the kinetic method described by Bergmeyer and Hørdler 1980 (Bio diagnostics, Cairo, Egypt), with a Roche P800 automatic biochemical analyzer (Roche, U.S.A.) [25].

Liver histopathological examination

Livers were dissected and fixed in a 10% phosphate-buffered paraformaldehyde solution. Tissues were dehydrated and embedded in paraffin and sectioned at $4\ \mu\text{m}$, stained with H&E, and then examined blindly under a light microscope. The severity and extent of steatosis were observed for each case. The findings were classified into the following degrees: grade (0): no change; grade (1): mild steatosis, occasional ballooning degeneration in zone 3, mild lobular inflammation with or without mild portal inflammation; grade

(2): moderate steatosis in 33–66% of lobules, ballooning degeneration in zone 3, moderate lobular inflammation with mild to moderate portal inflammation; grade (3): severe steatosis in > 66% of lobules, marked ballooning especially in zone 3, scattered lobular acute and chronic inflammation with moderate portal inflammation and perivascular and pericellular fibrosis limited to zone 3 [26].

Statistical analysis

Data are expressed as mean ± SD. The difference between groups was analyzed using one-way analysis of variance (ANOVA) and the Kruskal-Wallis test followed by Tukey's post-hoc test for multiple comparisons. The difference between group means was considered statistically significant when the *p*-value < 0.05. Data were analyzed using SPSS, version 17 (SPSS Inc., Chicago, Illinois, USA).

Results

There are no significant differences between the NPD and exenatide control group in regards to all the studied parameters.

Effect of ADF and/or exenatide on body weight

Weight of mice was assessed at the start and at the end of the experiment. HFD-fed animals' body weights were significantly higher than NPD-fed animals. The combined ADF and exenatide group showed lower weight when compared with the exenatide treated group (Figure 1 B; *p* < 0.05).

Effect of ADF and/or exenatide on lipid profile

Figure 2 shows a significant increase in the lipid profile parameters TC, TG, LDL, and VLDL but

a decrease in HDL in the HFD group compared to NPD treatment with ADF alone and the combined ADF + exenatide had reduced elevated lipid profile parameters and normalized HDL compared to the HFD group (*p* < 0.05). The same significant effect on TC, HDL, and LDL levels was also exerted by exenatide treatment (*p* < 0.05).

Effect of ADF and/or exenatide on leptin resistance

Effect of ADF and/or exenatide on brain leptin level and expression

Figure 3 shows that HFD was associated with higher brain leptin level (Figure 3 A) and mRNA expression of leptin receptors in comparison with the NPD control group (*p* < 0.05, Figure 3 B). Treatment with ADF and/or exenatide revealed effectiveness in reducing the leptin level and the expression of leptin receptors compared to the HFD control group. The combined ADF/exenatide treated group downregulated (*p* < 0.05) the high levels of leptin and leptin receptor expression compared to exenatide-treated group.

Effect of ADF and/or exenatide on brain leptin-sensitive cytokine receptor signaling: JAK2, STAT3, SOCS3 and PTP1B pathway

Figure 4 illustrates that expression of the leptin-sensitive proteins JAK2 (Figure 4 A) and STAT3 (Figure 4 B) was lower in HFD-fed mice in comparison to NPD-fed mice, with higher protein expression of the inhibitors SOCS3 (Figure 4 C) and PTP1B (Figure 4 D) (*p* < 0.05). Treatment with ADF and exenatide revealed effectiveness in increasing JAK2/STAT3 and inhibiting SOCS3 and PTP1B proteins in comparison with the HFD group and exenatide groups. It was more beneficial in upregulating the leptin-sensitive JAK2/STAT3 and

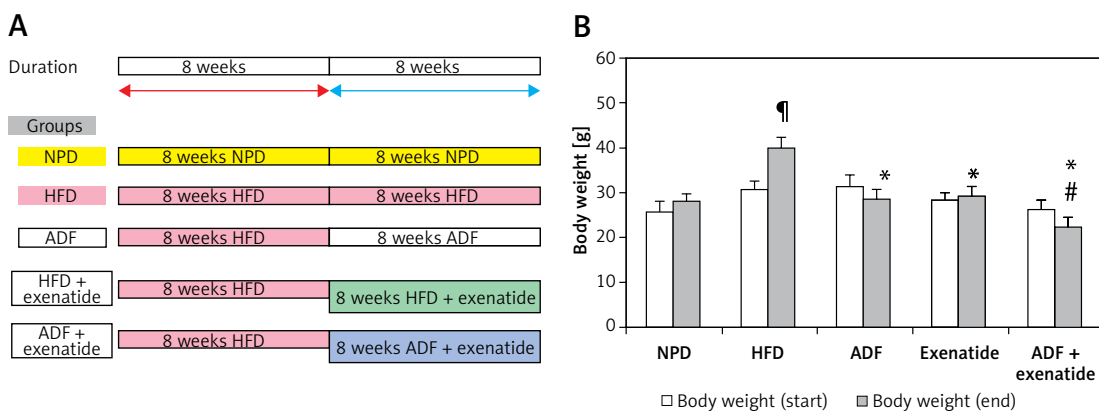


Figure 1. A – The dietary protocol. **B** – Mice's body weight at start and end of the study. Values are mean ± SD (*n* = 10), analyzed by one-way ANOVA followed by Tukey's multiple comparisons test. ^{*},^{*}*p* < 0.05; [#]compared with NPD control group, ^{*}compared with HFD control group, [#]compared with exenatide treated group

NPD – normal palatable diet, HFD – high-fat diet, ADF – alternate-day high-fat diet.

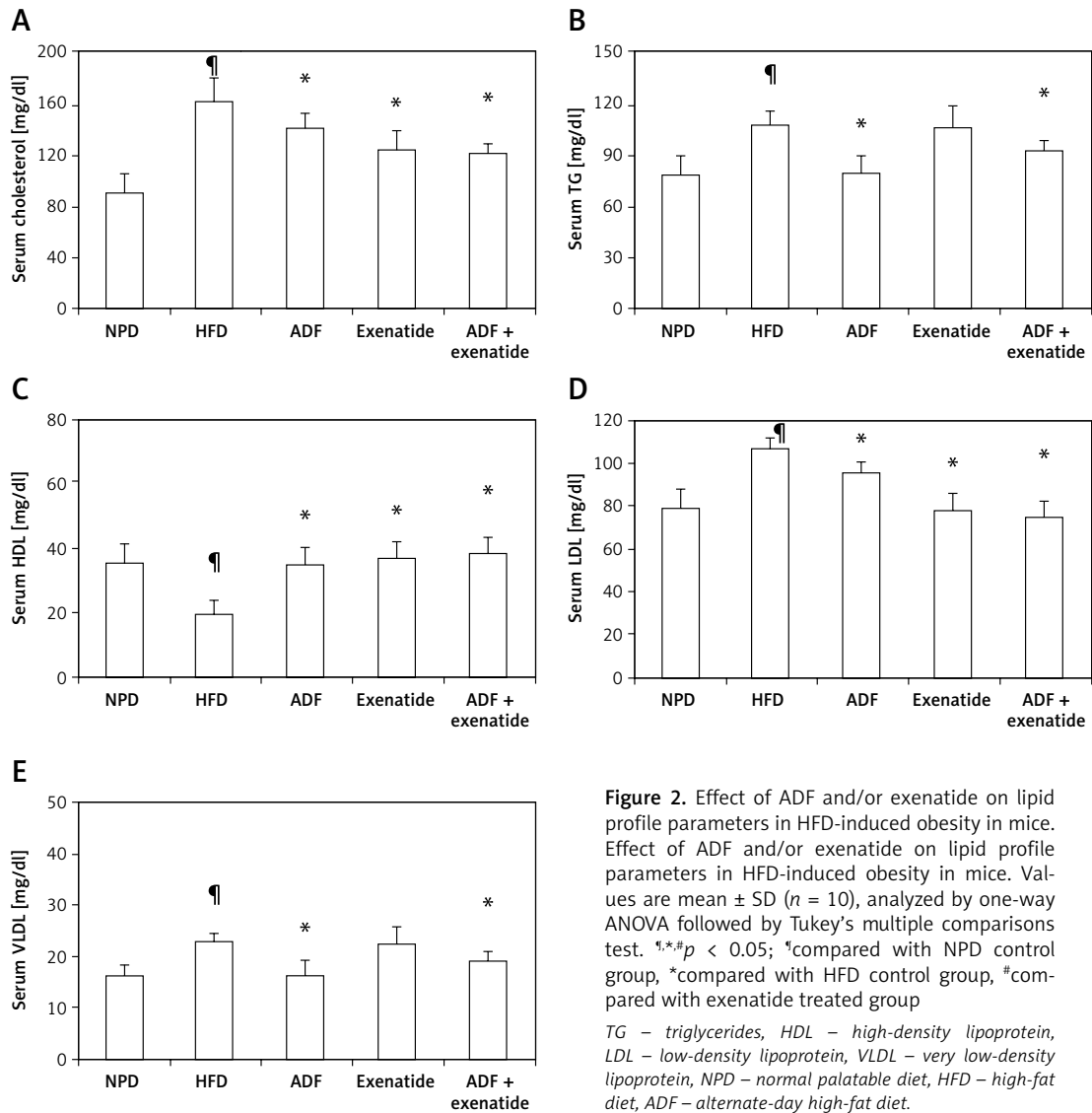


Figure 2. Effect of ADF and/or exenatide on lipid profile parameters in HFD-induced obesity in mice. Values are mean \pm SD ($n = 10$), analyzed by one-way ANOVA followed by Tukey's multiple comparisons test. [†],*[#] $p < 0.05$; ^{*}compared with NPD control group, ^{*}compared with HFD control group, [#]compared with exenatide treated group

TG – triglycerides, HDL – high-density lipoprotein, LDL – low-density lipoprotein, VLDL – very low-density lipoprotein, NPD – normal palatable diet, HFD – high-fat diet, ADF – alternate-day high-fat diet.

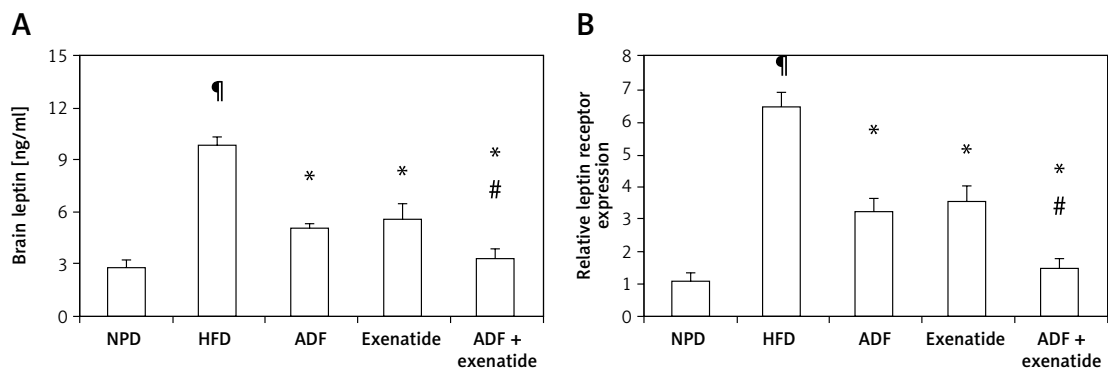


Figure 3. Effect of ADF and/or exenatide on brain leptin content and receptor expression in HFD-induced obesity in mice. High calorie fed obese mice showed HFD-enhanced brain leptin level and receptor expression. **A** – ELISA detected leptin “ng/ml”, **B** – qRT-PCR, relative expression of leptin receptor gene in HFD-induced leptin resistance in mouse brain. Values are mean \pm SD ($n = 10$), analyzed by one-way ANOVA followed by Tukey's multiple comparisons test. [†],*[#] $p < 0.05$; [†]compared with NPD control group, ^{*}compared with HFD control group, [#]compared with exenatide treated group

NPD – normal palatable diet, HFD – high-fat diet, ADF – alternate-day high-fat diet.

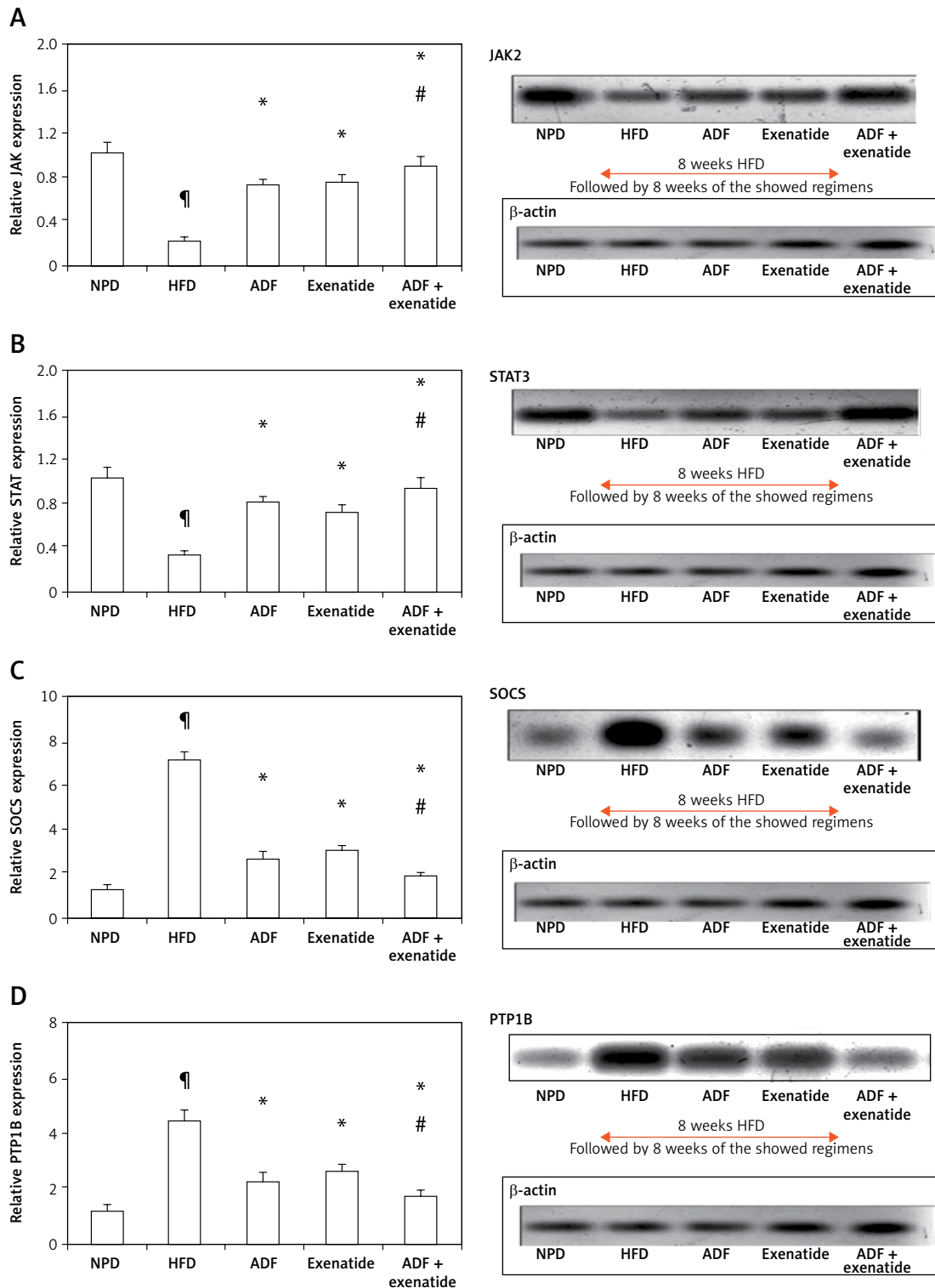


Figure 4. Effect of ADF and/or exenatide on brain leptin-related pathway protein expression levels in HFD-induced obesity in mice. Effect of ADF and exenatide on: **A** – JAK2; **B** – STAT3; **C** – SOCS, **D** – PTP1B protein expression levels in mice brain. Values are mean \pm SD ($n = 10$), analyzed by one-way ANOVA followed by Tukey's multiple comparisons test. *,# $p < 0.05$; *Compared with NPD control group, #compared with HFD control group, #compared with exenatide treated group

JAK2 – Janus kinase/signal transducer-2, STAT3 – activator of the transcription 3, SOCS – cytokine signaling 3, PTP1B – protein tyrosine phosphatase 1B, NPD – normal palatable diet, HFD – high-fat diet, ADF – alternate-day high-fat diet.

attenuating the severity of the activated SOCS3 and PTP1B signaling pathway compared to the exenatide treated group ($p < 0.05$, Figure 4) leading to decreased weight (Figure 1).

Effect of ADF and/or exenatide on insulin resistance

Effect of ADF and/or exenatide on insulin resistance markers

Figure 5 illustrates the elevation exerted by HFD, compared to the control group, on FBG (Figure 5 A), insulin (Figure 5 B) and HOMA-IR levels (Figure 5 C) to confirm the diabetic, insulin resistance model. A significant decrease in FBG is observed after the administration of ADF and/or exenatide. However, ADF combined with exenatide showed a statistically significantly lower FBG level compared to the exenatide treated group. Treatment with ADF and/or the GLP-1 agonist exenatide improved insulin level resistance and HOMA-IR ($p < 0.05$) compared to the HFD group.

Effect of ADF and/or exenatide on insulin signaling pathway

Figures 6 and 7 A show the effect of ADF and exenatide on mouse liver relative expression of insulin resistance genes IRS-1/PI3K/GLUT4 in HFD-induced obesity and insulin resistance liver mice. Liver IRS-1 (Figure 6 A), PI3K (Figure 6 B), and GLUT 4 (Figure 7 A) expression was lower in HFD-fed mice in comparison to NPD-fed mice. ADF and exenati-

de revealed effectiveness in increasing the expression of the IRS-1/PI3K/GLUT4 signaling pathway in comparison with the HFD group. Combined ADF and exenatide treatment was more beneficial in activation of the IRS-1/PI3K/GLUT4 genes signaling pathway compared to the exenatide treated group ($p < 0.05$), decreasing the fat deposit.

Effect of ADF and/or exenatide on hepatic steatosis markers

Effect of ADF and/or exenatide on hepatic adipogenicity genes

Figures 7 B and C demonstrate the effect of ADF and exenatide on the relative expression of adipogenicity genes *PDK3* and *NAFLD 2* expression in HFD-induced obesity and insulin resistance respectively, indicating higher mRNA expression in the HFD group in comparison, with NPD control, while the combined ADF and exenatide treated group downregulated the high levels of these genes compared to exenatide treated group ($p < 0.05$).

Effect of ADF and/or exenatide on liver enzymes

Figure 8 shows a significant reduction in ALT levels noted in the combined ADF and exenatide group with no improvement noted in the ADF group in comparison to the exenatide treated group ($p < 0.05$). No statistically significant difference is noted between the studied groups regarding levels of AST.

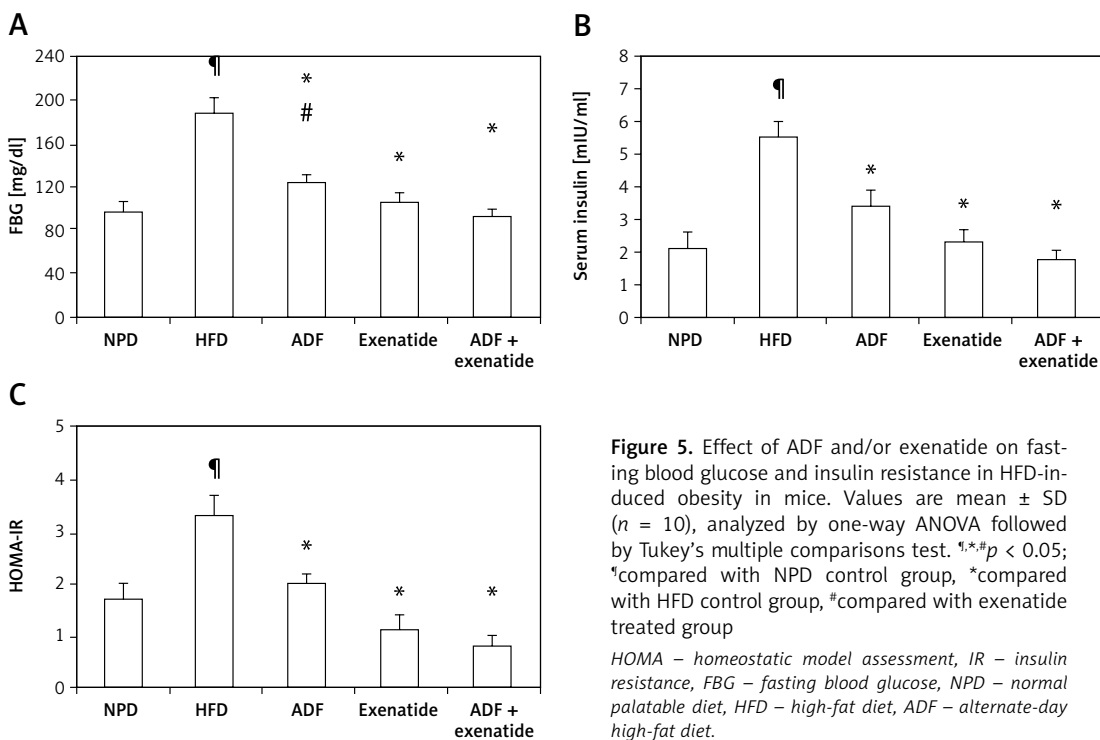


Figure 5. Effect of ADF and/or exenatide on fasting blood glucose and insulin resistance in HFD-induced obesity in mice. Values are mean \pm SD ($n = 10$), analyzed by one-way ANOVA followed by Tukey's multiple comparisons test. $^{\#}, *; p < 0.05$; $^{\#}$ compared with NPD control group, * compared with HFD control group, $^{\#}$ compared with exenatide treated group

HOMA – homeostatic model assessment, IR – insulin resistance, FBG – fasting blood glucose, NPD – normal palatable diet, HFD – high-fat diet, ADF – alternate-day high-fat diet.

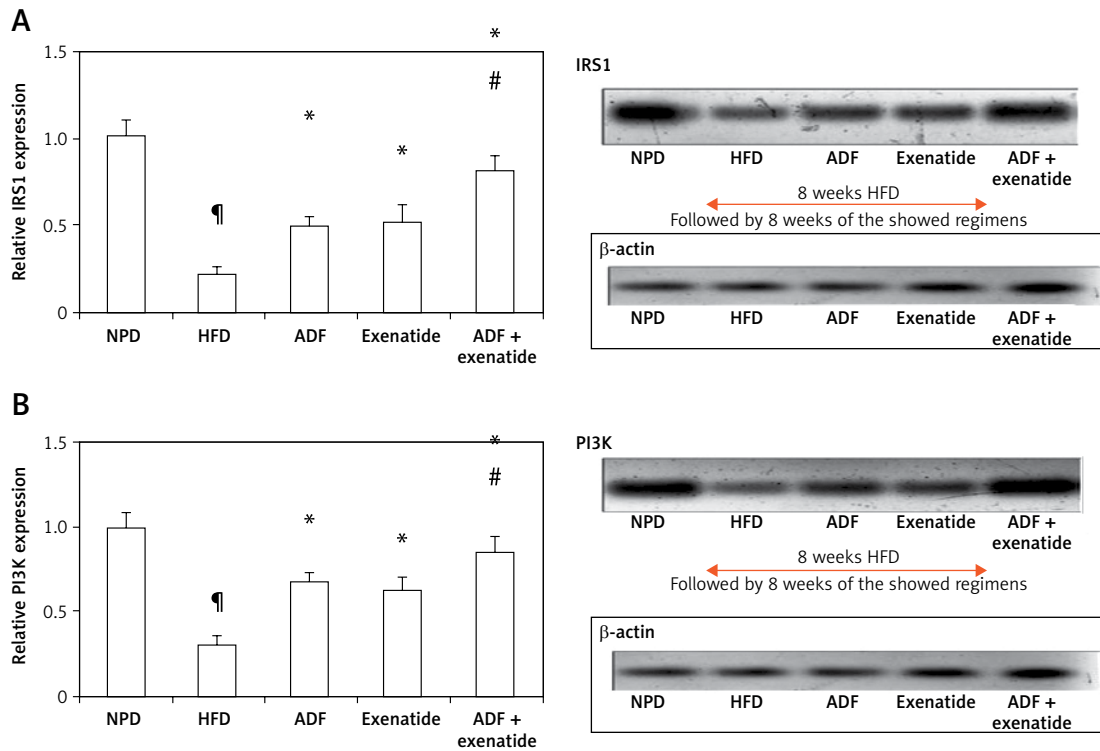


Figure 6. Effect of ADF and/or exenatide on liver insulin phosphorylation signal protein expression in HFD-induced obesity in mice. **A** – IRS1 is insulin transmitting signals to intracellular pathways. **B** – PI3K. Values are mean \pm SD ($n = 10$), analyzed by one-way ANOVA followed by Tukey's multiple comparisons test. *, # $p < 0.05$; *compared with NPD control group, #compared with HFD control group, #compared with exenatide treated group

IRS1 – insulin receptor substrate 1, PI3K – phosphatidylinositol 3-kinase, NPD – normal palatable diet, HFD – high-fat diet, ADF – alternate-day high-fat diet.

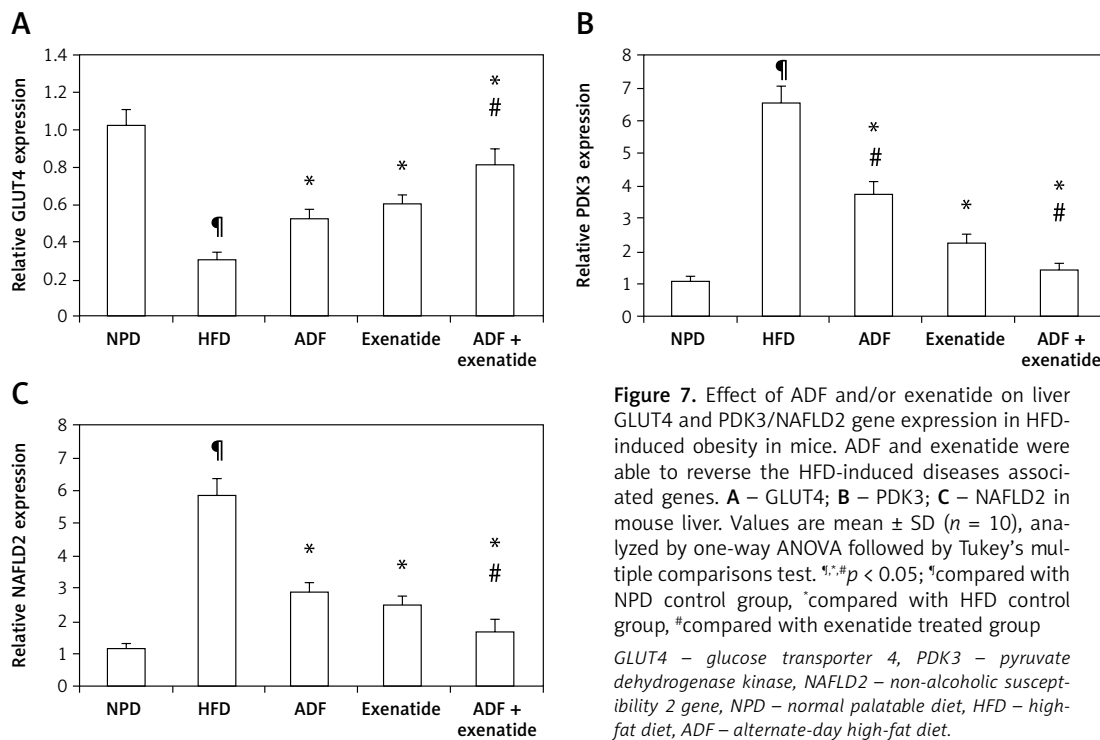


Figure 7. Effect of ADF and/or exenatide on liver GLUT4 and PDK3/NAFLD2 gene expression in HFD-induced obesity in mice. ADF and exenatide were able to reverse the HFD-induced diseases associated genes. **A** – GLUT4; **B** – PDK3; **C** – NAFLD2 in mouse liver. Values are mean \pm SD ($n = 10$), analyzed by one-way ANOVA followed by Tukey's multiple comparisons test. *, # $p < 0.05$; *compared with NPD control group, #compared with HFD control group, #compared with exenatide treated group

GLUT4 – glucose transporter 4, PDK3 – pyruvate dehydrogenase kinase, NAFLD2 – non-alcoholic susceptibility 2 gene, NPD – normal palatable diet, HFD – high-fat diet, ADF – alternate-day high-fat diet.

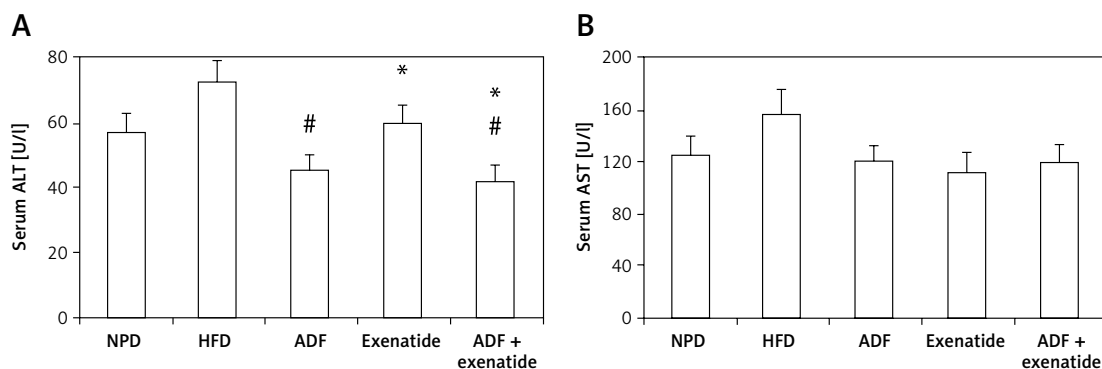


Figure 8. Effect of ADF and/or exenatide on liver enzymes in HFD- induced obesity in mice. Values are mean \pm SD ($n = 10$), analyzed by one-way ANOVA followed by Tukey's multiple comparisons test. # $p < 0.05$; *compared with NPD control group, *compared with HFD control group, #compared with exenatide treated group

ALT – alanine transaminase, AST – aspartate transaminase, NPD – normal palatable diet, HFD – high-fat diet, ADF – alternate-day high-fat diet.

Effect of ADF and/or exenatide on the hepatic histopathological picture

The histopathological examination (Figure 9) of the hepatic tissues revealed that the control group feeding on NPD as well as the NPD + exenatide groups showed preservation of the normal arrangement of hepatocytes (Figure 9 IA). However, hepatic tissues in HF-fed mice exhibited disturbed architecture (Figure 9 IB), with an increase in the mean histopathological score and percent area (%) in comparison with the NPD group ($p < 0.05$, Figures 9 II, III).

These deleterious effects associated with HFD were ameliorated by the administration of either ADF or exenatide (Figures 9 IC–E) with a reduction in the mean histopathological score in comparison with the HFD control group. However, treatment with combined ADF and exenatide was more beneficial in attenuating the severity of steatosis and improving the histopathological score and percent area compared with the exenatide-treated group ($p < 0.05$, Figures 9 II, III).

Discussion

ADF and/or exenatide significantly decreased the mice's body weight, similar to previous studies [27, 28]. Exenatide inhibits gastric motility and induces satiety, thus promoting weight reduction. However, the combined administration of ADF and exenatide revealed significantly lower weight when compared with the solitary administered ADF or exenatide groups. GLP-1 acts by decreasing hepatic free fatty acid uptake and reversing dyslipidemia [29]. Nevertheless, the combined regime did not differ from the solitary intervention of any of them in terms of reducing lipid profile parameters.

In the present study, HFD caused hyperleptinemia and leptin resistance by downregulating the JAK2/STAT3 signaling cascade and induced

SOCS3 and PTP1B expression. Similarly, Bian *et al.* observed that HFD promotes SOCS3 expression and the activation of STAT3 resistance by leptin in proopiomelanocortin neurons in rodents.

The current study demonstrated that the ADF/exenatide augmented the anorexic nervous system leptin-JAK2/STAT3 signaling and inhibited their suppressor SOCS3. In addition, the combined ADF and exenatide treatment was associated with decreased CNS leptin level and receptor expression, improving leptin resistance due to disturbance in the JAK2/STAT3 sensitivity to the self-regulated proteins SOCS3/PTP1B [30]. This could be attributed to the activated JAK2 autophosphorylation and consequently phosphorylation of tyrosine residues on the leptin receptor intracellular domain, allowing STAT proteins to bind with their subsequent nuclear translocation where they act as transcription factors and resulting in regaining of leptin's anorexigenic effects (suppression of appetite and induction of weight loss). Olofsson *et al.* reported that shifting from high-fat to low-fat diets decreases SOCS3 expression and ameliorates neuronal leptin resistance.

Regarding insulin sensitivity, it was obvious that treatment with ADF and/or the GLP-1 agonist exenatide ameliorated the elevated FBG and improved insulin levels and HOMA-IR, showing normalization of the insulin resistance picture developed by HFD. The combined ADF and exenatide treatment showed a further improvement in FBG levels. The combined regime did not differ from the solitary intervention of any of them in terms of the effect on the insulin level or HOMA-IR. One plausible explanation is the need for a longer period to normalize these metabolic disturbances.

Moreover, multiple signaling molecules (protein and kinases) are involved in the insulin signaling pathways that promote liver GLUT4 trafficking. One of these pathways is the IRS1/PI3K-medi-

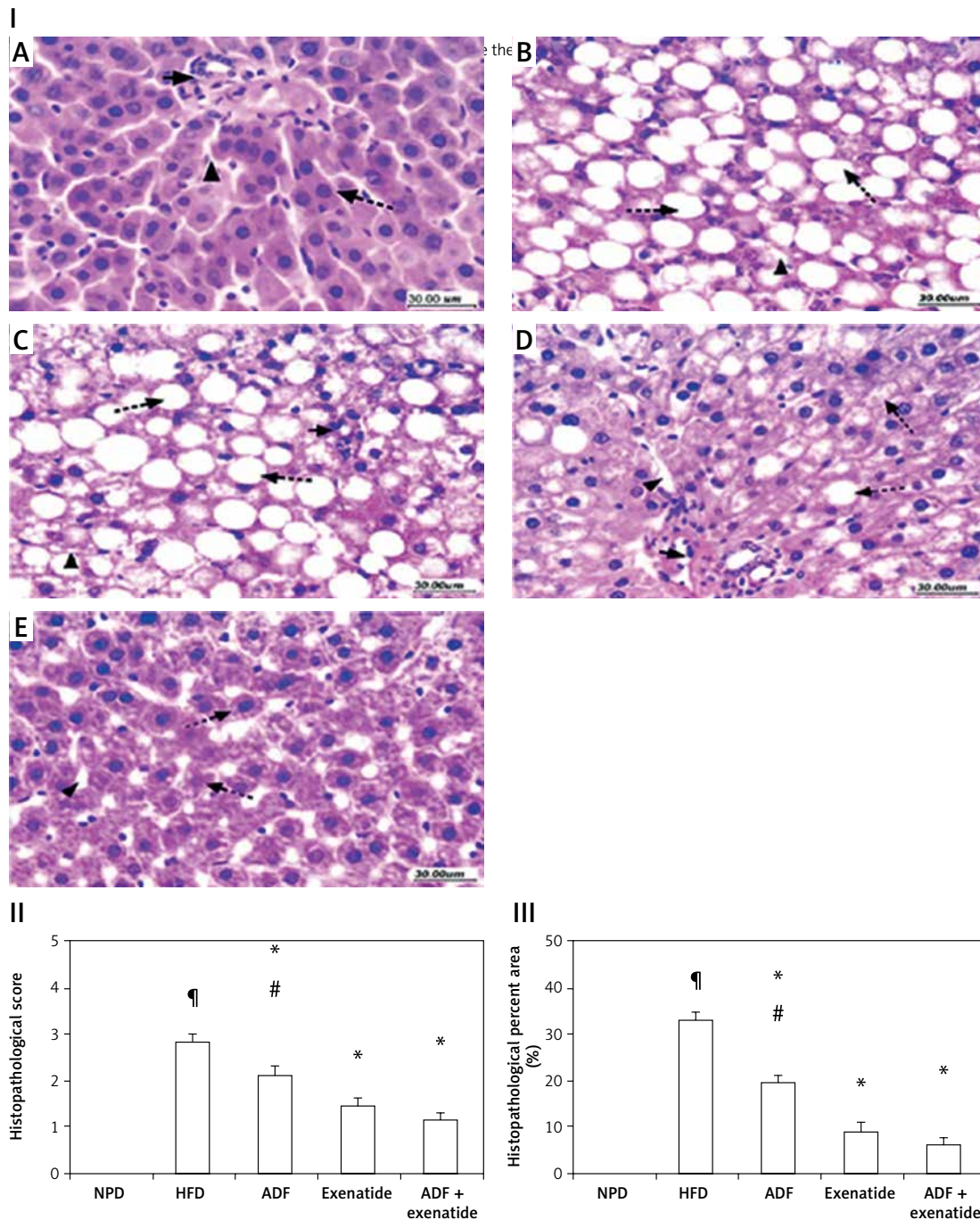


Figure 9. Effect of ADF and/or exenatide on hepatic histopathology in HFD-induced obesity in mice (I): Photomicrographs of hepatic sections stained with H&E for morphometric analysis. Sections from normal mice (A) showed preserved architecture with lobules formed of hepatocytes (dashed arrow) arranged in plates of one to two cell thickness showing abundant eosinophilic cytoplasm and central nucleus surrounded by blood sinusoids (arrow-head); portal areas (arrow) showed bile ductules and portal vessels. Sections from high diet fed mice (B) showed disturbed architecture with marked cytoplasmic clear vacuolation displacing nucleus (steatosis is more than 66%); there is also ballooning degeneration of some hepatocytes. Additionally, there is scattered lobular inflammatory cell infiltration (arrowhead). Mice' livers of ADF treated group (C) showed moderate ballooning degeneration and moderate focal steatosis; there is moderate portal inflammation with congested vessels. On the other hand, mice' livers of exenatide treated group (D) showed few hepatocytes with moderate ballooning degeneration; there is mild lobular focal inflammation with mild portal inflammation with few congested vessels. However, combined ADF and exenatide treated group (E) showed preserved architecture with lobules formed of hepatocytes arranged in thin plates showing abundant eosinophilic cytoplasm with residual focal mild ballooning degeneration and focal residual mild steatosis; there is no lobular inflammation (H & E 400×). II – Effect of ADF and/or exenatide on the histopathological score in HFD-induced obesity in mice. Values are mean ± SD ($n = 10$), analyzed by one-way ANOVA followed by Tukey's multiple comparisons test. *,# $p < 0.05$; #compared with NPD control group, *compared with HFD control group, #compared with exenatide treated group. III – Effect of ADF and/or exenatide on the histopathological percent area (%) in HFD-induced obesity in mice. Values are mean ± SD ($n = 10$), analyzed by one-way ANOVA followed by Tukey's multiple comparisons test. *,# $p < 0.05$; #compared with NPD control group, *compared with HFD control group, #compared with exenatide treated group

NPD – normal palatable diet, HFD – high-fat diet, ADF – alternate-day high-fat diet.

ated insulin signaling pathway, which becomes activated upon binding of insulin to its receptor, triggering translocation of GLUT4 from its storage vesicles to the plasma membrane [11]. The PI3K signaling cascade is strongly associated with insulin resistance incidence [30]. In the current study, hyperleptinemia and hyperinsulinemia abolished GLUT4 translocation through downregulation of the IRS1/PI3K/GLUT4 signaling pathway as shown in the HFD mouse group. In addition, elevated levels of the inhibitors SOCS3 and PTP1B could aggravate insulin resistance by suppressing the expression of IRS-1 (the main substrate in the insulin signaling pathway representing the main crosstalk point between insulin and leptin signaling pathways).

ADF combined with exenatide in the current study upregulates IRS1/PI3K/GLUT4 expression; this could improve the insulin receptor sensitivity, which could also be attributed to the suppressive effect exerted by the combined treatment on SOCS3 and PTP1B expression.

In agreement with the present study, Kim *et al.* (2014) observed a decrease in the hepatic GLUT4 expression in knock-out ob/ob mice, and the GLUT4 expression was increased by exenatide treatment [31]. Previous studies showed that exenatide exerts its antidiabetic effect mainly through the augmentation of insulin-dependent glucose uptake through GLUT4 translocation on the plasma membrane [11, 32]. Exenatide, via its insulin-dependent effect, can correct the worsened HFD diabetogenic impact on GLUT4 expression in liver cells [33].

Regarding its effect on liver steatosis, GLP-1 analogs ameliorate hyperlipidemia and liver steatosis and delay its progression to steatohepatitis [31], as observed in the current study, which can be linked to the effect exerted by the GLP-1 agonist exenatide on the overexpression of the leptin receptor signaling cascade and the improved leptin sensitivity. Hackl *et al.* (2019) demonstrated that brain leptin protects against hepatic steatosis by minimizing de novo lipogenesis beside the induction of triglyceride export through signaling in the dorsal vagal complex, where the efferent vagal motor neurons are located [34].

Consistently, the current study revealed the largest reduction in the HFD-induced expression of PDK3 associated with the combined ADF-exenatide treatment. PDK3 is one of the adipogenicity markers acting as a part of the pyruvate dehydrogenase complex (PDC), representing the central linker between glucose and lipid metabolism since the accumulation of fat droplets in the hepatocytes is the cornerstone in the pathogenesis of liver steatosis; it was concluded that deficiency of PDK3 improved liver steatosis [35]. Furthermore, this PDK3 downregulation was associated

with amelioration of expression of *NAFLD2*, one of the most recently described fatty liver disease associated genes, reversing the distorted hepatic histopathological picture seen in the HFD group with the degree of steatosis.

In conclusion, the current study demonstrated the beneficial effects of ADF combined with a GLP-1 agonist (exenatide) on the brain and liver. Centrally, ADF/exenatide reversed leptin resistance and its associated genes, including the JAK2/STAT3 signaling pathway, and attenuated the inhibitors SOCS3 and PTP1B, which consequently improved the insulin resistance-related genes, including liver IRS-1/PI3K/GLUT4, and boosted liver lipid export and improved hepatic steatosis via receptors expressed in the CNS. Therefore, high fat-diet induced obesity with leptin and insulin resistance and liver steatosis is manageable by ADF and the GLP-1 agonist exenatide.

Acknowledgments

The authors thank Prof Laila Rashed, Faculty of Medicine, Kasr El-Einy University, and Mohamed Kamal El-Kherbetawy, Faculty of Medicine, Suez Canal University for their help.

Conflict of interest

The authors declare no conflict of interest.

References

- Guzzardi MA, Guiducci L, Campani D, et al. Leptin resistance before and after obesity: evidence that tissue glucose uptake underlies adipocyte enlargement and liver steatosis/steatohepatitis in Zucker rats from early-life stages. *Int J Obes* 2022; 46: 50-8.
- Winzell MS, Ahrén B. The high-fat diet-fed mouse: a model for studying mechanisms and treatment of impaired glucose tolerance and type 2 diabetes. *Diabetes* 2004; 53 Suppl 3: S215-9.
- Ito M, Suzuki J, Tsujioka S, et al. Longitudinal analysis of murine steatohepatitis model induced by chronic exposure to high-fat diet: longitudinal analysis of diet-induced NASH model. *Hepatol Res* 2007; 37: 50-7.
- Havel PJ. Role of adipose tissue in body-weight regulation: mechanisms regulating leptin production and energy balance. *Proc Nutr Soc* 2000; 59: 359-71.
- Park HK, Ahima RS. Leptin signaling. *F1000Prime Rep* 2014; 6: 73.
- Ladyman SR, Grattan DR. JAK-STAT and feeding. *JAK-STAT* 2013; 2: e23675.
- Auernhammer CJ, Melmed S. The central role of SOCS-3 in integrating the neuro-immunoendocrine interface. *J Clin Invest* 2001; 108: 1735-40.
- Cho H. Protein tyrosine phosphatase 1B (PTP1B) and obesity. *Vitam Horm* 2013; 91: 405-24.
- Campbell JE, Drucker DJ. Pharmacology, physiology, and mechanisms of incretin hormone action. *Cell Metab* 2013; 17: 819-37.
- Arnés L, Moreno P, Nuche-Berenguer B, Valverde I, Villanueva-Peñacarrillo ML. Effect of exendin-4 treatment

- upon glucose uptake parameters in rat liver and muscle, in normal and type 2 diabetic state. *Regul Pept* 2009; 153: 88-92.
11. Kouidhi S, Berrhouma R, Rouissi K, et al. Human subcutaneous adipose tissue Glut 4 mRNA expression in obesity and type 2 diabetes. *Acta Diabetol* 2013; 50: 227-32.
 12. Zhang M, Zhao Y, Li Z, Wang C. Pyruvate dehydrogenase kinase 4 mediates lipogenesis and contributes to the pathogenesis of nonalcoholic steatohepatitis. *Biochem Biophys Res Commun* 2018; 495: 582-6.
 13. Petersen KF, Dufour S, Hariri A, et al. Apolipoprotein C3 gene variants in nonalcoholic fatty liver disease. *N Engl J Med* 2010; 362: 1082-9.
 14. Tawfik MK, Mohamed MI. Exenatide suppresses 1,2-dimethylhydrazine-induced colon cancer in diabetic mice: effect on tumor angiogenesis and cell proliferation. *Biomed Pharmacother* 2016; 82: 106-16.
 15. Srinivasan K, Viswanad B, Asrat L, Kaul CL, Ramarao P. Combination of high-fat diet-fed and low-dose streptozotocin-treated rat: a model for type 2 diabetes and pharmacological screening. *Pharmacol Res* 2005; 52: 313-20.
 16. Tawfik MK, El-Kherbetawy MK, Makary S. Cardioprotective and anti-aggregatory effects of levosimendan on isoproterenol-induced myocardial injury in high-fat-fed rats involves modulation of PI3K/Akt/mTOR signaling pathway and inhibition of apoptosis: comparison to cilostazol. *J Cardiovasc Pharmacol Ther* 2018; 23: 456-71.
 17. Vila-Bedmar R, Cruces-Sande M, Arcones AC, et al. GRK2 levels in myeloid cells modulate adipose-liver crosstalk in high fat diet-induced obesity. *Cell Mol Life Sci* 2020; 77: 4957-76.
 18. Smith NJ, Caldwell JL, van der Merwe M, et al. A comparison of dietary and caloric restriction models on body composition, physical performance, and metabolic health in young mice. *Nutrients* 2019; 11: 350.
 19. Saad ZA, Khodeer DM, Zaitone SA, Ahmed AAM, Moustafa YM. Exenatide ameliorates experimental non-alcoholic fatty liver in rats via suppression of toll-like receptor 4/NF κ B signaling: comparison to metformin. *Life Sci* 2020; 253: 117725.
 20. Elshaer RE, Tawfik MK, Nosseir N, et al. Leflunomide-induced liver injury in mice: involvement of TLR4 mediated activation of PI3K/mTOR/NF B pathway. *Life Sci* 2019; 235: 116824.
 21. Livak KJ, Schmittgen TD. Analysis of relative gene expression data using real-time quantitative PCR and the 2- $\Delta\Delta$ CT method. *Methods* 2001; 25: 402-8.
 22. Srinivasan K, Viswanad B, Asrat L, Kaul CL, Ramarao P. Combination of high-fat diet-fed and low-dose streptozotocin-treated rat: a model for type 2 diabetes and pharmacological screening. *Pharmacol Res* 2005; 52: 313-20.
 23. Allain CC, Poon LS, Chan CSG, Richmond W, Fu PC. Enzymatic determination of total serum cholesterol. *Clin Chem* 1974; 20: 470-5.
 24. Fossati P, Prencipe L. Serum triglycerides determined colorimetrically with an enzyme that produces hydrogen peroxide. *Clin Chem* 1982; 28: 2077-80.
 25. Yang W, Cao M, Mao X, et al. Alternate-day fasting protects the livers of mice against high-fat diet-induced inflammation associated with the suppression of Toll-like receptor 4/nuclear factor κ B signaling. *Nutr Res* 2016; 36: 586-93.
 26. Angulo P. Nonalcoholic fatty liver disease. *N Engl J Med* 2002; 346: 1221-31.
 27. Folli F, Guardado Mendoza R. Potential use of exenatide for the treatment of obesity. *Expert Opin Investig Drugs* 2011; 20: 1717-22.
 28. Acosta A, Camilleri M, Burton D, et al. Exenatide in obesity with accelerated gastric emptying: a randomized, pharmacodynamics study. *Physiol Rep* 2015; 3: e12610.
 29. Russell S. Incretin-based therapies for type 2 diabetes mellitus: a review of direct comparisons of efficacy, safety and patient satisfaction. *Int J Clin Pharm* 2013; 35: 159-72.
 30. Zhang M, Wang X, Liu M, et al. Inhibition of PHLPP1 ameliorates cardiac dysfunction via activation of the PI3K/Akt/mTOR signalling pathway in diabetic cardiomyopathy. *J Cell Mol Med* 2020; 24: 4612-23.
 31. Kim S, Jung J, Kim H, et al. Exendin-4 improves nonalcoholic fatty liver disease by regulating glucose transporter 4 expression in ob/ob mice. *Korean J Physiol Pharmacol* 2014; 18: 333-9.
 32. Andreozzi F, Raciti GA, Nigro C, et al. The GLP-1 receptor agonists exenatide and liraglutide activate glucose transport by an AMPK-dependent mechanism. *J Transl Med* 2016; 14: 229.
 33. Chen LN, Lyu J, Yang XF, et al. Liraglutide ameliorates glycometabolism and insulin resistance through the upregulation of GLUT4 in diabetic KKAY mice. *Int J Mol Med* 2013; 32: 892-900.
 34. Hackl MT, Fürsinn C, Schuh CM, et al. Brain leptin reduces liver lipids by increasing hepatic triglyceride secretion and lowering lipogenesis. *Nat Commun* 2019; 10: 2717.
 35. Zhang M, Zhao Y, Li Z, Wang C. Pyruvate dehydrogenase kinase 4 mediates lipogenesis and contributes to the pathogenesis of nonalcoholic steatohepatitis. *Biochem Biophys Res Commun* 2018; 495: 582-6.